

---

# DEEP NEURAL NETWORKS FOR THE CORRECTION OF MIE SCATTERING IN FOURIER-TRANSFORMED INFRARED SPECTRA OF BIOLOGICAL SAMPLES

---

A PREPRINT

Arne P. Raulf    Joshua Butke    Lukas Menzen    Claus Küpper    Frederik Großerueschkamp

Klaus Gerwert

Axel Mosig

Center for Protein Diagnostics  
Ruhr-University Bochum  
Gesundheitscampus 4  
44801 Bochum, Germany  
axel.mosig@bph.rub.de

February 19, 2020

## ABSTRACT

Infrared spectra obtained from cell or tissue specimen have commonly been observed to involve a significant degree of (resonant) Mie scattering, which often overshadows biochemically relevant spectral information by a non-linear, non-additive spectral component in Fourier transformed infrared (FTIR) spectroscopic measurements. Correspondingly, many successful machine learning approaches for FTIR spectra have relied on preprocessing procedures that computationally remove the scattering components from an infrared spectrum.

We propose an approach to approximate this complex preprocessing function using deep neural networks. As we demonstrate, the resulting model is not just several orders of magnitudes faster, which is important for real-time clinical applications, but also generalizes strongly across different tissue types. Furthermore, our proposed method overcomes the trade-off between computation time and the corrected spectrum being biased towards an artificial reference spectrum.

## 1 Introduction

Fourier transform infrared (FTIR) spectroscopic imaging of biological samples provides pixel spectra at high spatial resolution which carry a highly informative fingerprint of the biochemical status of the sample. FTIR microscopy thus has been applied successfully in characterizing the disease state of tissue samples of different types from several different organs [9, 7]. However, the raw spectra obtained from FTIR imaging experiments inherently suffer from the Mie scattering effect [12, 11], which affects the measured absorption spectra and complicates the data analysis [1].

The underlying scattering effect is observable when applying FTIR imaging to biological samples. Here, cells, nuclei or other cellular components within a certain size range [12, 11] lead to a Mie scattering effect. This model led to the development of first correction procedures [8] based on the *extended multiplicative signal correction* algorithm [10]. This approach was extended by the authors of [2], who introduced an iterative correction procedure for resonant Mie scattering (RMieS). While this approach takes into account scattering only, it has recently been further improved upon by approximating the complete Mie extinction through complex valued refractive indices of the scatterers [15]. In short, an FTIR pixel spectrum observed in an hyperspectral microscopic image is a mixture of Mie scattering and

resonant absorption factors, which has led to the development of correspondingly complex computational correction procedures.

While the very recent ME-EMSC approach [15] promises great improvement over the less elaborate scattering model of the RMieS approach, our contribution is focused on the latter approach [2], which has been popular in a large range of studies [7, 9, 17]. Throughout this manuscript, we will refer to the approach from [2] as *RMieS correction*. This approach employs a reference spectrum, which represents an idealized baseline of a scattering-free infrared spectrum. This spectrum is used iteratively to approximate the measured, distorted spectra to the pure absorbance spectrum using the *extended multiplicative signal correction* [2]. Because of its iterative nature there is a strong trade-off of between time and accuracy to reach satisfactory results, making it computationally expensive.

In a recent contribution, we demonstrated that in the presence of sufficient data for training, deep neural networks may circumvent RMieS correction algorithm [13]. This approach is based on an approach introduced in the context of *representation learning* [4], specifically by employing the approach introduced in [14] to perform unsupervised pre-training followed by supervised fine-tuning to classify pixel spectra into a discrete set of classes, i.e., tissue components.

While the neural network introduced in [13] involves training data obtained from RMieS corrected spectra and thus involves RMieS correction in an implicate manner, the model possesses no explicit knowledge of Mie scattering. Yet, it has been hypothesized in [13] that, due to the strong generalization capability of the network, it may have learned to disentangle the raw spectra into an abstract representation that separates scattering from the molecular spectrum. Our present contribution further investigates this hypothesis by explicitly training the network to approximate the complex function computed by the RMieS correction procedure. The rationale behind our present study is roughly as follows: We replace the final layer of a pretrained classifying neural network by a regression layer to learn RMieS correction – if supervised finetuning of the pretrained regression network successfully learns RMieS correction, this provides evidence about the disentanglement in the classifying network, namely that the pretraining helps to disentangle those variances that are due to resonant Mie scattering.

## 2 Methods

### 2.1 Dataset

For our study, we used data sets from [13] and [7] that we briefly recapitulate for the sake of completeness. All samples were recruited from thin-sections of colon cancer associated tissue samples. Two types of tissue were used. Our first set of samples was recruited from formalin fixed paraffin embedded (FFPE) histopathological samples, and the second set from fresh frozen (FF) tissue. The samples were further subdivided into one dataset FFPE<sub>pt</sub> for pretraining (see Section 3), and one dataset FFPE<sub>ft</sub> for supervised training (finetuning) the regression-model. The tissue microarray data from [13] were used for training using an identical subdivision into training and validation data as described in [13]. Whole-slide images from [7] were used as independent test sets.

## 3 Approach

Our general approach is to extend the stacked autoencoder based network topology and training procedure from [13] for classifying infrared pixel spectra to obtain a neural network that approximates the RMieS correction procedure from [3], as illustrated in Figure 1. In fact, we used the RMieS correction implementation described in [3] to produce training and validation data; to introduce some essential notation, we denote an RMieS corrected spectrum  $y = R(x)$ , where  $R$  denotes the RMieS correction procedure and  $x$  an uncorrected raw spectrum from one of the data sets.

Specifically, we use the paradigm of unsupervised pretraining as established in [6, 14], where an unsupervised pretraining on unlabeled data is used to give the initial mode for the used weight matrices in further training stages. While in [13], these pretrained models underwent supervised finetuning to train a classifier network, this present contribution deals with a regression network aiming to approximate the RMieS correction function rather than aiming to classify pixel spectra. In other words, we deal with a neural network whose output layer represents Mie-corrected infrared spectra. To this end, we replace the transfer function of the output layer from a softmax function commonly used for classifying networks to a linear activation function suiting the requirements of a regression model. All regression models are based on an unsupervised Contractive Stacked Autoencoder (CSAE) [14] which was trained only on the FFPE<sub>pt</sub> dataset. Throughout the paper, we will use  $\theta$  to denote the parameters obtained from supervised finetuning, and  $y = S_{\theta}(x)$  the network with parameters  $\theta$  applied to input spectrum  $x$ , i.e., the approximation of the corrected spectrum of  $x$ . During training, we used root mean square error as loss function.

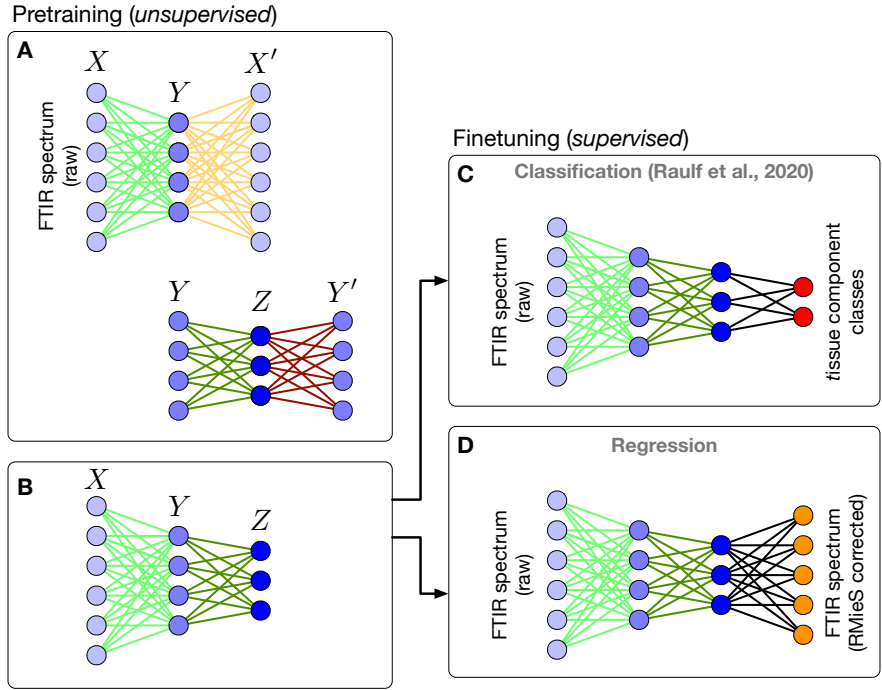


Figure 1: Overview of our approach to train a regression network (panel **D**) that approximates RMieS correction based on unsupervised pretraining through stacked autoencoders (panels **A** and **B**). The approach is similar to the tissue component classifier proposed in [13] (panel **C**) Each output neuron of the regression network (indicated in orange in panel **D**) learns regression of one specific wavenumber of the RMieS corrected spectrum.

### Validation Measures

We validate our trained model  $\theta$  on each of the validation data sets  $F$  at three levels. At the first level, we investigate the root mean square error  $RMSE_{\theta} = \sum_{x \in F} \|R(x) - S_{\theta}(x)\|$ . On a second level of validation, we used an existing random forest based classifier  $C$  from a previous study [9] that classifies a Mie corrected spectrum  $y$  into one out of nineteen different tissue component classes  $C(y)$ , and compared the output classes of the ground truth  $C(R(x))$  with the classification obtained from an approximated correction, i.e.,  $C(S_{\theta}(X))$ . We will refer to the classifier  $C$  as a *downstream* model and thus refer to this validation approach as *downstream validation*.

On a third level of validation, we assess uncertainty of the trained regression model based on the Bayesian dropout approach proposed by Gal *et al* [5], which systematically integrates the concept of *dropout layers* (i.e., the randomized dropping of neurons in specific layers) into an approximation of a Gaussian process. The statistical processes can be introduced into trained neural networks by using the usual dropout [16] not only as a tool to prevent overfitting on the training dataset but also during the test phase to randomly exclude 50% of neurons at test time. By excluding neurons at test time, one obtains a Bernoulli distribution over all different models of the trained network, which approximates the variational inference and finally approximates the deep Gaussian process. The latter step yields a tool to interpret deep neural networks as models by considering the prediction itself, the mean of the prediction and the variance of this process.

The RMieS correction procedure is also highly time sensitive, which led us to validate the running time difference between the RMieS correction reference implementation and its neural network approximator. As an iterative approach that needs to be applied to each individual pixel spectrum in an infrared microscopic image, practical running times can amount to hours when dealing with whole slide images that comprise tens of millions of pixel spectra [7], where several iterations of the RMieS correction procedure may be required to achieve high quality corrected spectra. At the same time, it is not straightforward to implement the RMieS correction algorithm in a way that the parallelization capability of graphics hardware can be fully exploited [3]. Here, the potential promise of an approximator network is a large increase in processing speed, since common neural network frameworks can inherently and fully exploit parallelization capability.

Model	EMSC	NN
Time for val.-set	64.99 sec	10.65 sec
Time per spectrum	118.23 $\mu$ sec	28.96 $\mu$ sec

Table 1: Running times obtained from RMieS correction reference implementation (*EMSC*) and the approximation by neural network (*NN*) for a data set size of 360000 spectra. Recorded times were averaged over 10 runs each.

**Implementation** We utilized two implementations of the RMieS correction provided by the authors of [2]. Henceforth, we will refer to these implementations as *EMSC V2* and *EMSC V5*, respectively. The network  $S_\theta$  was trained using raw spectra as input and *EMSC V2* corrected spectra as target output for regression learning. The *EMSC V5* implementation was used as a reference. All neural networks were implemented using the Theano framework, as described in [13].

## 4 Results

**Downstream validation.** Figure 2 shows the comparison of the validation dataset for the FFPE data using the random forest introduced in [9] as downstream classifier that classifies RMieS corrected spectra into one out of 19 different tissue components. Compared to the ground truth segmentation obtained from  $C(R(x))$  for each pixel spectrum  $x$ , the approximation based classification constituted by  $C(S_\theta(x))$  achieves an accuracy of 78% across all pixels in the whole-slide image displayed in Figure 3.

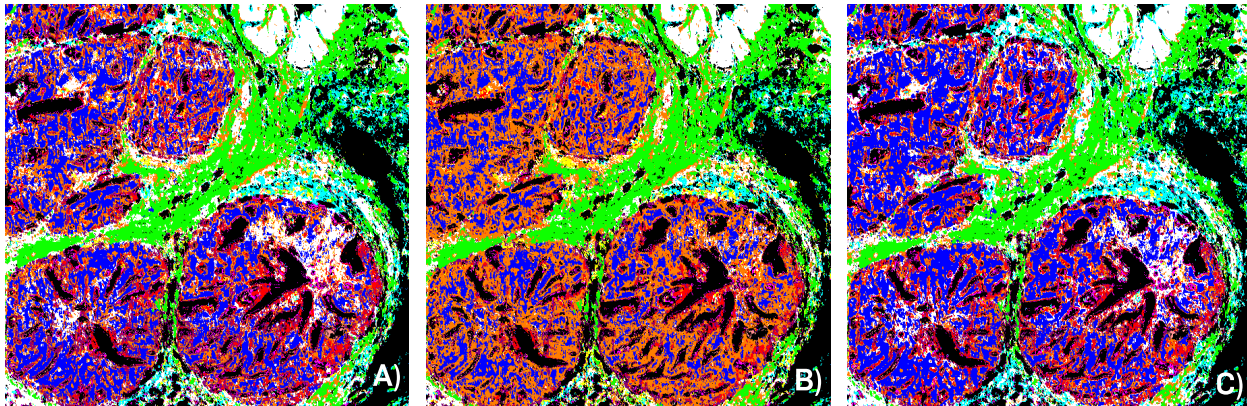


Figure 2: Panel **A** displays classification results of the random forest classifier from [9] applied to the FTIR spectra corrected with the *EMSC V2* implementation of the RMieS correction. Panel **B** displays classification results obtained from the same classifier, but spectra corrected using the *EMSC V5* implementation of the FTIR spectra [7]. Panel **C** displays spectra corrected by the regression network  $S_\theta$  that was trained to approximate the correction as implemented in *EMSC V2*.

**Running time.** To assess running times, we performed correction of a validation data set of size  $600 * 600$  spectra. The time that has been recorded was averaged over 10 different runs each and are summarized in the Table 1.

### Characterization of approximation capabilities.

As indicated in Figure 4 and panel **C** of Figure 5, the corrected spectra obtained from network  $S_\theta$  approximate the RMieS correction function with only little error. However, the deviation around the amide I peak around  $1650 \text{ cm}^{-1}$  is remarkably high. In fact, detailed inspection (Figure 5) indicates a band shift between the RMieS corrected ground truth spectrum and the neural network approximation. To further assess this band shift, we performed Bayesian dropout validation, which yields a confidence interval at each wavenumber, as displayed in Figure 6. The confidence intervals are strikingly large around the amide I peak. In other words, the band shift coincides with a low-confidence region of the network.

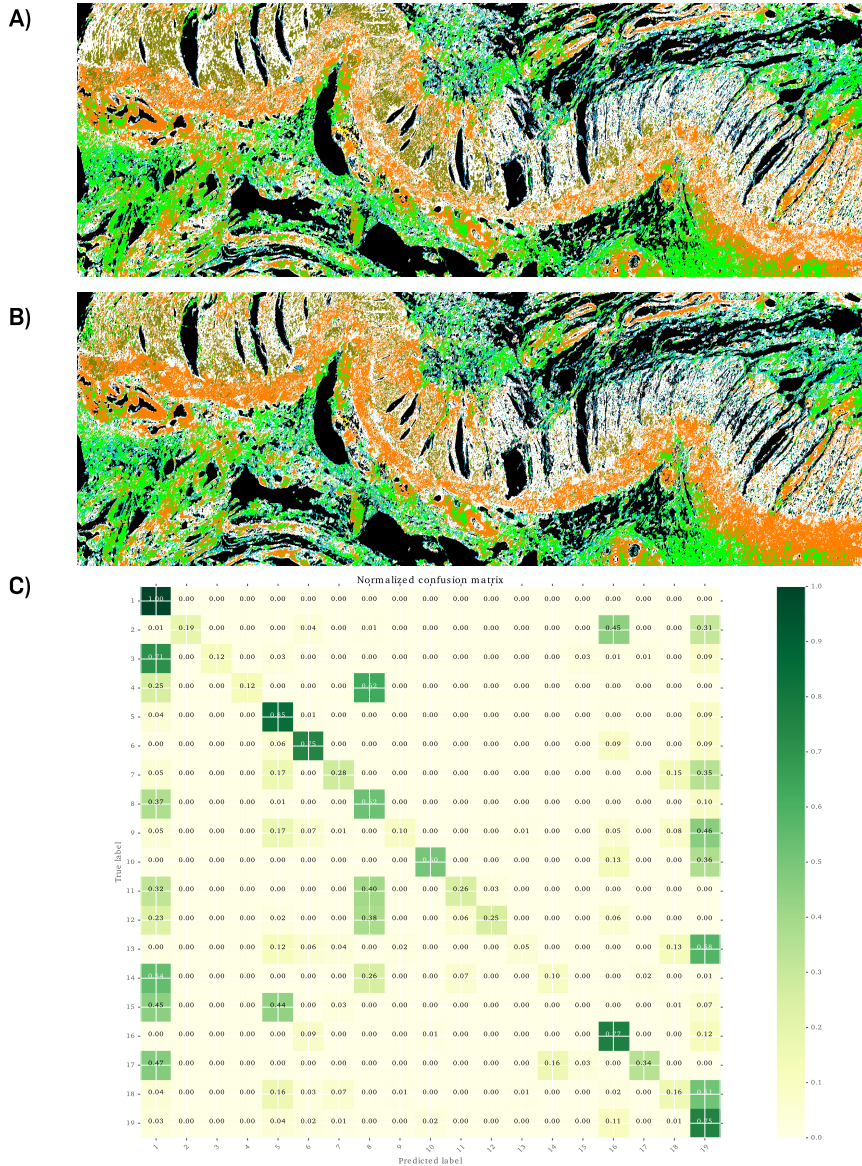


Figure 3: Panel A displays classification results of the random forest classifier from [9] applied to the FTIR spectra corrected with the *EMSC V2* implementation of the RMieS correction. Panel B displays spectra corrected by the regression network  $S_\theta$  that was trained to approximate the correction as implemented in *EMSC V2*. A normalized confusion matrix is displayed in panel C.

## 5 Conclusion

Our results clearly demonstrate that the RMieS correction for infrared spectra can be approximated by a neural network that produces practically useful corrected spectra, while using only a fraction of the computation time. Beyond the immediate and practically highly relevant benefit in terms of computational speedup, our results also contribute to the understanding and interpreting of what deep neural network models have learned during supervised training. In fact, in [13] it was hypothesised that autoencoder-based pretraining for a *classifying* neural network may have learned to disentangle raw infrared pixel spectra in a manner such that the variance due to resonant Mie scattering has been separated from the variance that is due to vibrations at the molecular level. The fact that the same pretrained stacked autoencoder allows to compute corrected spectra adds further support to this hypothesis.

In general, it is important to keep in mind the inherent limitations of approximations obtained from deep neural networks as the one we have introduced here. In fact, the network function  $S_\theta$  we obtain is a very local approximation

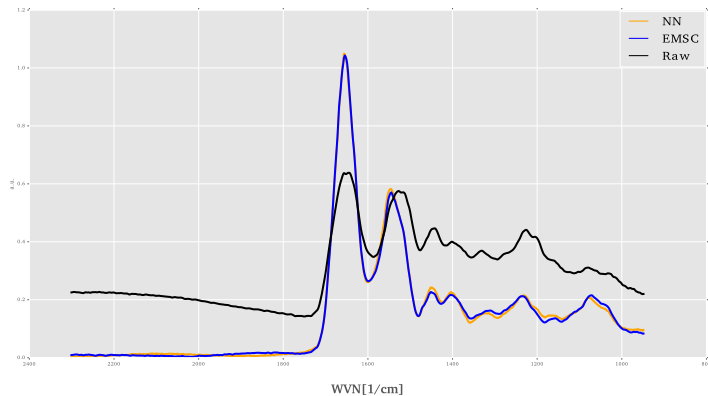


Figure 4: Example of an FTIR spectrum from FFPE tissue, shown as raw spectrum (black), corrected by the RMieS correction algorithm from [2] (blue) and corrected by the neural network  $S_\theta$  that approximates the RMieS correction. EMSC.

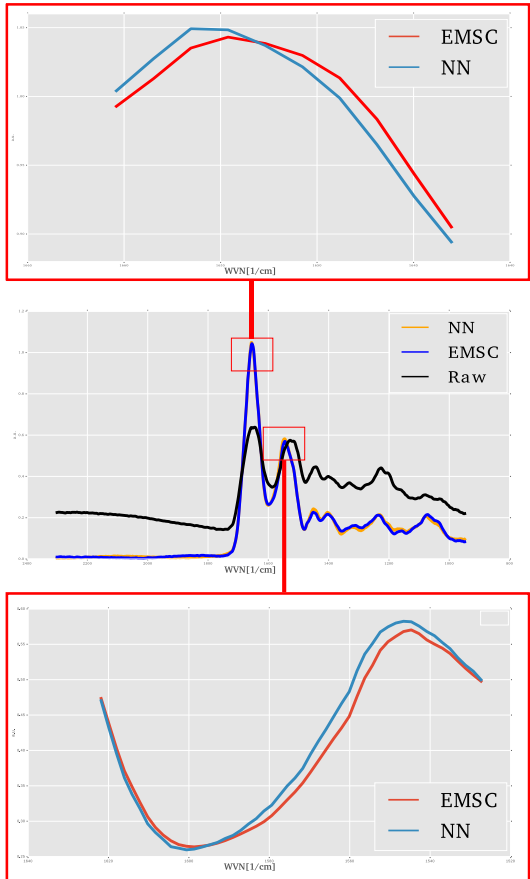


Figure 5: Comparison of band shift by reference implementation of RMieS correction (*EMSC*) and the approximating neural network (*NN*).

of the RMieS correction function  $R$  in the sense that it works primarily for input spectra that sufficiently resemble the training data. In other words, as long as a raw spectrum  $x$  is obtained from FFPE samples of colon tissue, applied to similar substrate and spectroscopically measured in a similar manner, then  $S_\theta(x)$  will produce spectra that will reliably resemble  $R(x)$ . It is a highly relevant question for future research to train networks that work reliably on a broader set

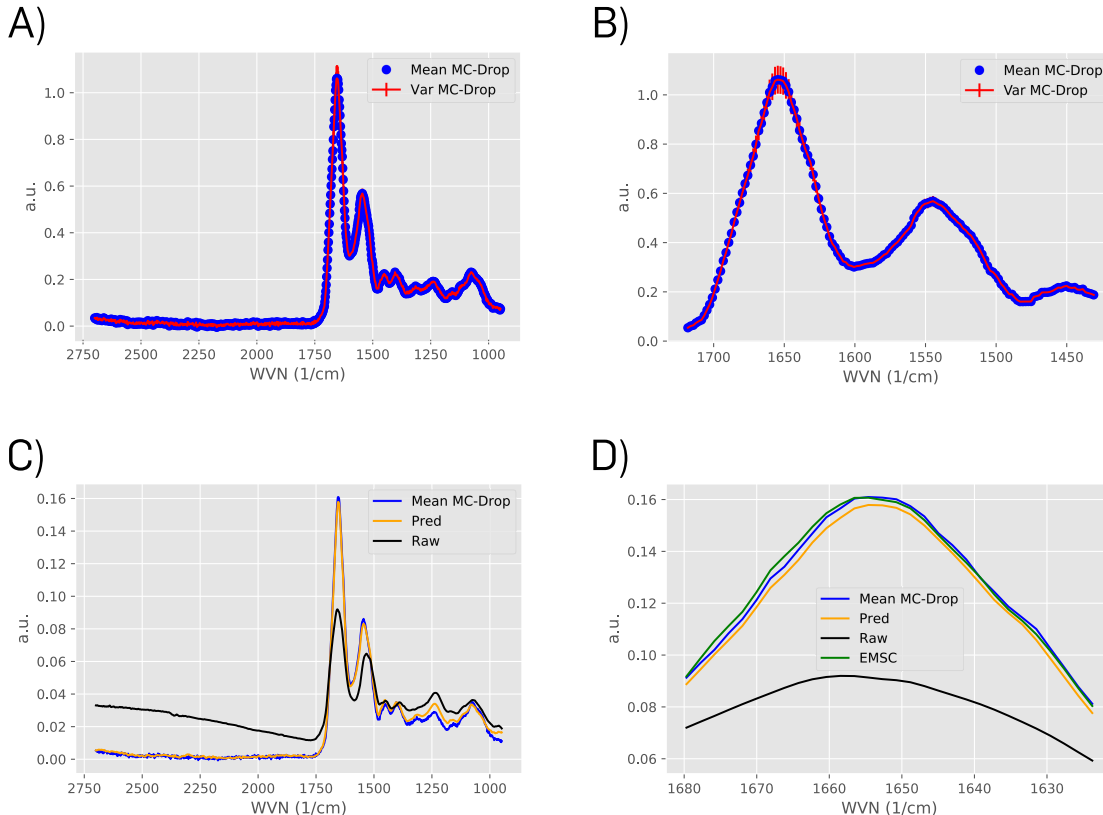


Figure 6: *Panel A*: Mean spectrum obtained by neural network  $S_\theta$  including confidence interval obtained by MC dropout; *Panel B*: Same as *A*, focusing on the Amide bands of the spectrum and demonstrating the relatively low confidence in the regression around the amide I peak; *Panel C*: Comparison of mean spectra; *Panel D*: Same as *C*, focusing on the Amide bands of the spectrum.

of inputs, e.g. across tissue from different organs and being either FFPE or fresh-frozen as well as potentially being prepared on different substrate material.

Even with the limited generalization guarantee resulting from relatively limited training data, the computational speedup constitutes a factor that makes our results promising from a practical perspective, since the high demand of computation time can easily become a road block in many practical setting, when e.g. dealing with whole slide images.

## References

- [1] P. Bassan, H. J. Byrne, F. Bonnier, J. Lee, P. Dumas, and P. Gardner. Resonant mie scattering in infrared spectroscopy of biological materials – understanding the ‘dispersion artefact’. *Analyst*, 134:1586–1593, 2009.
- [2] P. Bassan, A. Kohler, H. Martens, J. Lee, H. J. Byrne, P. Dumas, E. Gazi, M. Brown, N. Clarke, and P. Gardner. Resonant mie scattering (rmies) correction of infrared spectra from highly scattering biological samples. *Analyst*, 135(2):268–277, 2010.
- [3] P. Bassan, A. Kohler, H. Martens, J. Lee, E. Jackson, N. Lockyer, P. Dumas, M. Brown, N. Clarke, and P. Gardner. Rmies-emsc correction for infrared spectra of biological cells: Extension using full mie theory and gpu computing. *Journal of biophotonics*, 3(8-9):609–620, 2010.
- [4] Y. Bengio, A. Courville, and P. Vincent. Representation learning: A review and new perspectives. *IEEE transactions on pattern analysis and machine intelligence*, 35(8):1798–1828, 2013.
- [5] Y. Gal and Z. Ghahramani. Dropout as a bayesian approximation: Representing model uncertainty in deep learning. In *international conference on machine learning*, pages 1050–1059, 2016.

- 
- [6] G. E. Hinton and R. R. Salakhutdinov. Reducing the dimensionality of data with neural networks. *science*, 313(5786):504–507, 2006.
- [7] A. Kallenbach-Thieltges, F. Großerüschkamp, A. Mosig, M. Diem, A. Tannapfel, and K. Gerwert. Immunohistochemistry, histopathology and infrared spectral histopathology of colon cancer tissue sections. *Journal of biophotonics*, 6(1):88–100, 2013.
- [8] A. Kohler, J. Sule-Suso, G. Sockalingum, M. Tobin, F. Bahrami, Y. Yang, J. Pijanka, P. Dumas, M. Cotte, D. Van Pittius, et al. Estimating and correcting mie scattering in synchrotron-based microscopic fourier transform infrared spectra by extended multiplicative signal correction. *Applied spectroscopy*, 62(3):259–266, 2008.
- [9] C. Kuepper, F. Großerueschkamp, A. Kallenbach-Thieltges, A. Mosig, A. Tannapfel, and K. Gerwert. Label-free classification of colon cancer grading using infrared spectral histopathology. *Faraday discussions*, 187:105–118, 2016.
- [10] H. Martens and E. Stark. Extended multiplicative signal correction and spectral interference subtraction: new preprocessing methods for near infrared spectroscopy. *Journal of pharmaceutical and biomedical analysis*, 9(8):625–635, 1991.
- [11] M. Miljković, B. Bird, and M. Diem. Line shape distortion effects in infrared spectroscopy. *Analyst*, 137(17):3954–3964, 2012.
- [12] B. Mohlenhoff, M. Romeo, M. Diem, and B. R. Wood. Mie-type scattering and non-beer-lambert absorption behavior of human cells in infrared microspectroscopy. *Biophysical journal*, 88(5):3635–3640, 2005.
- [13] A. P. Raulf, J. Butke, C. Küpper, F. Großerueschkamp, K. Gerwert, and A. Mosig. Deep representation learning for domain adaptable classification of infrared spectral imaging data. *Bioinformatics*, 36(1):287–294, 2020.
- [14] S. Rifai, P. Vincent, X. Muller, X. Glorot, and Y. Bengio. Contractive auto-encoders: Explicit invariance during feature extraction. 2011.
- [15] J. H. Solheim, E. Gunko, D. Petersen, F. Großerüschkamp, K. Gerwert, and A. Kohler. An open-source code for mie extinction extended multiplicative signal correction for infrared microscopy spectra of cells and tissues. *Journal of biophotonics*, 12(8):e201800415, 2019.
- [16] N. Srivastava, G. Hinton, A. Krizhevsky, I. Sutskever, and R. Salakhutdinov. Dropout: a simple way to prevent neural networks from overfitting. *The journal of machine learning research*, 15(1):1929–1958, 2014.
- [17] K. E. Witzke, F. Großerueschkamp, H. Jütte, M. Horn, F. Roghmann, N. von Landenberg, T. Bracht, A. Kallenbach-Thieltges, H. Käfferlein, T. Brüning, et al. Integrated fourier transform infrared imaging and proteomics for identification of a candidate histochemical biomarker in bladder cancer. *The American journal of pathology*, 189(3):619–631, 2019.